Copy2 R61
ACCN:215268
RAL-92-033

Science and Engineering Research Council
Rutherford Appleton Laboratory
Chilton DIDCOT Oxon OX11 0QX

RAL-92-033

***** RAL LIBRARY R61 *****
Acc_No: 215268
Shelf: RAL R61 92033

Nonlinear Response Function Estimation: IV Generalised Auto Regression and Chaos

A D Irving and T Dewson

LIBRARY, R61
15 JUN 1992
RUTHERFORD APPLETON LABORATORY

May 1992

Science and Engineering Research Council
"The Science and Engineering Research Council does not accept any responsibility for loss or damage arising from the use of information contained in any of its reports or in any communication about its tests or investigations"

NONLINEAR RESPONSE FUNCTION ESTIMATION: IV GENERALISED AUTO REGRESSION AND CHAOS

A D Irving* and T Dewson +

*Energy Research Unit, Rutherford Appleton Laboratory, Chilton, Didcot, Oxon OX11 0QX UK

+Department of Mechanical Engineering, Queens Building, The University of Bristol, University Walk, Bristol BS8 1TR, UK

ABSTRACT

A formalism for the diagnostic analysis of time series from nonlinear physical processes is developed. The dynamics of nonlinear systems can be characterised in terms of response functions. The properties of delayed nonlinear mappings and nonlinear autoregression are discussed. A response function representation is adopted and a formalism is developed which uses higher order time series moments to estimate their values from the data. The properties of the formalism are illustrated by three examples. First, the accuracy of the method and its ability to identify the order and form of the mapping is demonstrated using a delayed logistic map. Then Wolf's annual sunspot number, which is theoretically predicted to be a delayed logistic map, is analysed and discussed. Finally, data from a driven electronic anharmonic oscillator which exhibits period doubling and chaotic behaviour is analysed and discussed.

INTRODUCTION

There are a large number of physical systems which exhibit nonlinear and chaotic behaviour. Naturally one wishes to characterise the data and analyse the physics underlying the process. However, the temporal evolution of these systems renders the quantitative analysis of such data extremely difficult in general. Many of the analysis techniques applied to experimental data are based on the linear time series analysis methods such as the correlation [1-3] and its Fourier transform the spectral density [4-9] or alternatively on maximum likelihood methods [10, 11]. In the latter case one has to guess the form of the model and fit the data to that model and the number of parameters that can realistically be fitted is severely limited [10]. Much effort has been devoted to the application of linear time series techniques and the interpretation of the results from the analysis using these techniques. Such analyses are straightforward but are difficult to interpret and are inconsistent and their use should be questioned. When considering the problem of prediction and forecasting from the observed time series [11-13] local predictors [14] or autoregressive models [2] with a small number of parameters are usually employed. Although such models can replicate aspects of the observed qualitative behaviour of any particular set of data they can be inconsistent and fail to yield the detailed quantitative information required for the development of empirical theories.

In this paper the focus is on the analyses of single sequences of time series data in terms of nonlinear response functions.

Much attention for the past decade has been directed to the iterative map [15]

$$x(t) = f(x(t-1))$$

and more recently the delayed logistic map [16]

$$x(t) = a(0)x(t-1)(1-x(t-1)) + \sum_{\sigma_i=1}^{\mu} a(i)x(t-\sigma_i)$$

where μ is the memory of the mapping.

In this work the general mapping

$$x(t) = \sum_{n=1}^{N} \frac{1}{n!} \sum_{\sigma_1=1}^{\mu} \cdots \sum_{\sigma_n=1}^{\mu} g_n(\sigma_1,\ldots,\sigma_n) \prod_{i=1}^{n} x(t-\sigma_i)$$

and the nonlinear autoregression representation

$$x(t) = r(t) + \sum_{n=1}^{N} \frac{1}{n!} \sum_{\sigma_1=1}^{\mu} \cdots \sum_{\sigma_n=1}^{\mu} g_n(\sigma_1,\ldots,\sigma_n) \prod_{i=1}^{n} x(t-\sigma_i)$$

are considered. A formalism, based on statistical moments, is developed that can estimate the nonlinear response function values $g_n(\sigma_1,\ldots,\sigma_n)$ from experimental data.

A numerical simulation is used to demonstrate the ability of the formalism to accurately determine the response values for an initial value chaotic map with memory but no noise. The formalism is then used to analyse two experimental data sets. The first data set to be analysed is Wolf's annual sunspot number which has been hypothesised to be governed by a delayed logistic map [17]. The second data set to be analysed is the observed voltage values from a nonlinear anharmonic electrical resonator which is known to follow a bifurcation route to chaos [4, 18].

GENERALISED AUTO REGRESSION AND CHAOS

Time series analysis is primarily concerned with the modelling of the linear properties of random functions. The most general linear relationship between adjacent time steps in terms of the history of the sequence $\{x(t)\}$ and the response function $g_1(t)$ is the convolution equation

$$x(t) = \sum_{\sigma_1=1}^{\mu} g_1(\sigma_1)x(t-\sigma_1) + r(t) \qquad (1)$$

where r(t) is an independent externally induced noise term. Equation (1) is often called an autoregressive representation [2]. The autoregressive representation assumes that $\{x(t)\}$ contains both deterministic and stochastic components. In this work it is assumed that the process has a finite memory of duration μ units and this should not be confused with the apparent memory of the data which may seem infinite.

Given a time series sequence of observations $x(1),\ldots,x(t) = \{x(t)\}$ then a typical representation would be

$$x(t) = \theta(t) + r(t) \tag{2}$$

where $\theta(t)$ is considered to be a deterministic function and r(t) a stochastic or noise function. Equation (2) represents a decomposition of the observed series into two theoretical components which one tries to separate and estimate from the data. The techniques used to analyse the data should in principle be able to discriminate between the origins of the different phenomena [19] but there will not be a unique solution to this decomposition.

When the mapping is nonlinear and when there is no noise, then, x(t) may be written in terms of a Volterra series expansion. That is, in terms of the time history of $\{x(t)\}$ and the response functions [20] $g_n(\sigma_1,\ldots,\sigma_n)$. In discrete form a nonlinear mapping may be defined as

$$x(t) = \sum_{n=1}^{N} \frac{1}{n!} \sum_{\sigma_1=1}^{\mu} \cdots \sum_{\sigma_n=1}^{\mu} g_n(\sigma_1,\ldots,\sigma_n) \prod_{j=1}^{n} x(t-\sigma_j) \tag{3}$$

which may be seen to be a form of Volterra series and is a straightforward generalisation of the linear autoregression method given in equation (1). Equation (3) represents a mapping between the sequence of data points without any noise term.

Taking absolute moments of Equation (3) we have that

$$\left\langle \prod_{j=1}^{m} x(t-\tau_j)x(t) \right\rangle = \sum_{n=1}^{N} \frac{1}{n!} \sum_{\sigma_1=1}^{\mu} \cdots \sum_{\sigma_n=1}^{\mu} g_n(\sigma_1,\ldots,\sigma_n)$$

$$\left\langle \prod_{j=1}^{m} x(t-\tau_j) \prod_{i=1}^{n} x(t-\sigma_i) \right\rangle \qquad (4)$$

This gives a set of simultaneous nonlinear integral equations with

$$\begin{bmatrix} M_{xx}(\tau_1,0) \\ M_{x^2x}(\tau_1,\tau_2,0) \\ \vdots \\ M_{x^Nx}(\tau_1,..,\tau_N,0) \end{bmatrix} = \begin{bmatrix} M_{xx}(\tau_1,\sigma_1) & \cdots & M_{xx^N}(\tau_1,\sigma_1,\ldots,\sigma_N) \\ \vdots & & \vdots \\ M_{x^Nx}(\tau_1,..,\tau_N,\sigma_1) & \cdots & M_{x^Nx^N}(\tau_1,..,\tau_N,\sigma_1,..\sigma_N) \end{bmatrix} \circledast \begin{bmatrix} g_1(\sigma_1) \\ \vdots \\ g_N(\sigma_1,..,\sigma_N) \end{bmatrix}$$

(5)

with τ_i, $\sigma_j > 0$. These equations can be solved for the unknown response values $g_n(\sigma_1,\ldots,\sigma_n)$ using standard matrix methods [21]. The formalism developed here is applicable when the moments of $\{x(t)\}$ are well defined.

The map $x(t+1) = f(x,t)$, often associated with chaotic dynamics [15], this map can be seen to be a special case of the above. For example, consider a process $\{x(t)\}$ where the memory can be characterised with only one coefficient, such that

$$x(t) = \sum_{n=1}^{N} \frac{1}{n!} \sum_{\sigma_1=1}^{\mu} \cdots \sum_{\sigma_n=1}^{\mu} g_n(\sigma_1,\ldots,\sigma_n) \prod_{j=1}^{n} \delta(\sigma_j=1)\, x(t-\sigma_j) \qquad (6)$$

Then this may be compared to the generalised bifurcation formalism [15]

$$x(t) = \sum_{p=1}^{N} b(p)\, x^{p}(t-1) \qquad (7)$$

and by inspection the coefficients b(p) may be related to the response functions by

$$b(p) = \frac{1}{p!}\, g_p(\sigma_1,\ldots,\sigma_p) \prod_{i=1}^{p} \delta(\sigma_i=1) \ . \qquad (8)$$

In the limit the response functions $g_p(\sigma_1,\ldots,\sigma_p)$ have been reduced to a simple delta functional form. This describes the system in terms of nonlinear gain parameters b(p), but because of the delta functions, $\delta(\tau_i)$, this representation does not describe the dynamics of the process. It is usual to consider the data to have an infinite memory; however, if the map $x(t) \rightarrow x(t+1)$ is thought of as an input output system and if the nonlinear system is approximately memoryless then the coefficients b(p) represent the nonlinear gain for each power p. Alternatively it may be that the nonlinear process has a finite memory, but that the data are observed at intervals which are long compared to the response times of the process. In that case the data points $\{x(t)\}$ are actually disconnected and any characterisation obtained will be of an envelope of spot values for which the causal link has been broken. The data should be collected at a time interval that is short or comparable with the response time so that the physical properties of the process may be identified, characterised and analysed.

The mapping given in Equation (3) is not in its most general form as the effects of 'noise' have been neglected. Such 'noise' may arise because of the stochastic nature of the driving force, or because of instrumentational effects, or because more than a single process is being observed. It is usual to assume that $\{r(t)\}$ is drawn from a Gaussian white noise distribution and is independent of the deterministic mapping $\{x(t)\}$, in this case

$$z(t) = r(t) + \sum_{n=1}^{N} \frac{1}{n!} \sum_{\sigma_1=1}^{\mu} \cdots \sum_{\sigma_n=1}^{\mu} g_n(\sigma_1,\ldots,\sigma_n) \prod_{i=1}^{n} x(t-\sigma_i) \qquad (9)$$

where $\{z(t)\}$ is the observed sequence of data. That is, the observed time series $\{z(t)\}$ has been theoretically decomposed into a deterministic component $\{x(t)\}$ and a stochastic component $\{r(t)\}$. The estimated values of the mapping $g_n(\sigma_1,\ldots,\sigma_n)$ will of course be dependent on the choice of $\{r(t)\}$ and its properties. The response functions $g_n(\sigma_1,\ldots,\sigma_n)$ will not be unique and are unlikely to yield detailed quantitative insight into the physics underlying the process.

Taking absolute moments of $\{z(t)\}$ we have that

$$\left\langle \prod_{j=1}^{m} z(t-\tau_j) z(t) \right\rangle = \left\langle \prod_{j=1}^{m} z(t-\tau_j) r(t) \right\rangle$$

$$+ \sum_{n=1}^{N} \frac{1}{n!} \sum_{\sigma_1=1}^{\mu} \cdots \sum_{\sigma_n=1}^{\mu} g_n(\sigma_1,\ldots,\sigma_n) \left\langle \prod_{j=1}^{m} z(t-\tau_j) \prod_{i=1}^{n} \{z(t-\sigma_i)-r(t-\sigma_i)\} \right\rangle \qquad (10)$$

The set of simultaneous equations given by (10) have to be solved for the mapping values $g_n(\sigma_1,\ldots,\sigma_n)$; in addition, they must be solved for some properties of the stochastic distribution $\{r(t)\}$.

The set of equations to be solved is

$$\begin{vmatrix} M_{zz}(1,0) \\ M_{zz}(\tau_1,0) \\ \vdots \\ M_zN_z(\tau_1,\ldots,\tau_N) \end{vmatrix} =$$

$$\begin{vmatrix} M_{zr}(0,0) & M_{zz}(0,\sigma_1) \ldots\ldots\ldots\ldots & M_zN_z(0,\sigma_1,\ldots,\sigma_N) \\ M_{zr}(\tau_1,0) & M^*_{zz}(\tau_1,\sigma_1) \ldots\ldots\ldots\ldots & M^*_zN_z(\tau_1,\sigma_1,\ldots,\sigma_N) \\ \vdots & \vdots & \vdots \\ M_zN_r(\tau_1,\ldots,\tau_N,0) & M^*_{zz}N(\tau_1,\ldots,\tau_N,\sigma_1) \ldots & M^*_zN_zN(\tau_1,\ldots,\tau_N,\sigma_1,\ldots,\sigma_N) \end{vmatrix}$$

$$\circledast \begin{vmatrix} 1.0 \\ g_1(\sigma_1) \\ \vdots \\ g_N(\sigma_1,\ldots,\sigma_N) \end{vmatrix} \qquad (11)$$

where the $M^*_zi_zj(\tau_1,\ldots,\tau_i,\sigma_1,\ldots,\sigma_j)$ contain mixed terms between $\{r(t)\}$ and $\{z(t)\}$.

Equation (11) may be considerably simplified if, without loss of generality, it is assumed that $\{r(t)\}$ is a zero mean Gaussian white noise process and that $\{x(t)\}$ is statistically independent to $\{r(t)\}$. Under this approximation we may write, for example, the equations for the N = 2 quadratic map case as

$$\begin{vmatrix} M_{zz}(1,0) \\ M_{zz}(\tau_1,0) \\ M_z{}^2{}_z(\tau_1,\tau_2,0) \end{vmatrix} = \begin{vmatrix} 1.0 & M_{zz}(0,\sigma_1) & M_z{}^2{}_z(0,\sigma_1,\sigma_2) \\ 0.0 & M^*_{zz}(\tau_1,\sigma_1) & M^*_z{}^2{}_z(\tau_1,\sigma_1,\sigma_2) \\ 0.0 & M^*_{zz}{}^2(\tau_1,\tau_2,\sigma_1) & M^*_z{}^2{}_z{}^2(\tau_1,\tau_2,\sigma_1,\sigma_2) \end{vmatrix} \circledast \begin{vmatrix} M_{rr}(0) \\ g_1(\sigma_1) \\ g_2(\sigma_1,\sigma_2) \end{vmatrix} \quad (12)$$

where the adjusted moment values are given by

$$M^*_{zz}(\tau_1,\sigma_1) = M_{zz}(\tau_1,\sigma_1) - M_{rr}(0)\ \delta(\tau_1=\sigma_1)$$

$$M^*_{zz}{}^2(\tau_1,\sigma_1,\sigma_2) = M_{zz}{}^2(\tau_1,\sigma_1,\sigma_2)$$
$$-\{M_z(\tau_1)\delta(\sigma_1=\sigma_2)+M_z(\sigma_1)\delta(\tau_1=\sigma_2) + M_z(\sigma_2)\delta(\tau_1=\sigma_1)\}\ M_{rr}(0)$$

$$M^*_z{}^2{}_z(\tau_1,\tau_2,\sigma_1) = M_z{}^2{}_z(\tau_1,\tau_2,\sigma_1)$$
$$-\{M_z(\tau_1)\delta(\sigma_1=\tau_2)+M_z(\tau_2)\delta(\sigma_1=\tau_1)\}\ M_{rr}(0)$$

and

$$M^*_z{}^2{}_z{}^2(\tau_1,\tau_2,\sigma_1,\sigma_2) = M_z{}^2{}_z{}^2(\tau_1,\tau_2,\sigma_1,\sigma_2)$$
$$+\{2M_{rr}(0)-M_{zz}(\tau_1,\sigma_1)\delta(\tau_2=\sigma_2)-M_{zz}(\tau_1,\sigma_2)\delta(\tau_2=\sigma_1)$$
$$-M_{zz}(\tau_2,\sigma_1)\delta(\tau_1=\sigma_2)-M_{zz}(\tau_2,\sigma_2)\delta(\tau_1=\sigma_1)\}M_{rr}(0) \quad (13)$$

which may be solved by substitution iteration or maximum likelihood methods for the values of $M_{rr}(0)$ and $g_n(\tau_1,\ldots,\tau_n)$. As the variance of the noise $M_{rr}(0)$tends to zero, equation (11) reduces to equation (5).

NUMERICAL ANALYSIS EXAMPLE OF A CHAOTIC SEQUENCE

In this section the results from a numerical experiment are presented where the properties of the nonlinear system are known. A numerical experiment is used so that the accuracy and range of appropriate use for the method in estimating the nonlinear response values and their predictive power can be assessed.

The data sequences were generated using the convolution equation

$$x(t) = \sum_{\tau_1=1}^{\mu'} g_1'(\tau_1)x(t-\tau_1) + \sum_{\tau_1=1}^{\mu'} g_2'(\tau_1,\tau_2)x(t-\tau_1)x(t-\tau_2) \qquad (14)$$

In this delayed logistic map example a random initial condition is selected for the sequence and some 2000 points of data, $\{x(t)\}$ are generated. The data $\{x(t)\}$ were then used to estimate the nonlinear response values. The estimated nonlinear response values $g_1(\tau_1)$ and $g_2(\tau_1,\tau_2)$ are then compared against the known responses $g_1'(\tau_1)$ and $g_2'(\tau_1,\tau_2)$, hence the accuracy and range of appropriate use of the method may be established. The accuracy of the nonlinear response function estimate is determined by the root mean square (rms) difference between the known and estimated nonlinear response values. The accuracy of the predictive power is determined by the normalised root mean square (nrms) difference between the actual and predicted output time series sequences.

Where the rms value is determined for the first order or linear response, using

$$\text{rms} = \left\{ \frac{1}{(\mu+1)} \sum_{\tau_1=1}^{\mu} (g_1(\tau_1) - g_1'(\tau_1))^2 \right\}^{\frac{1}{2}}$$

and for the second order or quadratic response

$$\text{rms} = \left\{ \frac{1}{(\mu+1)^2} \sum_{\tau_1=1}^{\mu} \sum_{\tau_2=1}^{\mu} (g_2(\tau_1,\tau_2) - g_2'(\tau_1,\tau_2))^2 \right\}^{\frac{1}{2}}$$

where μ is the memory of the process.

The normalised root mean square difference between the original data set $\{x(t)\}$ and the predicted data $\{x_p(t)\}$ is

$$\text{nrms} = \left\{ \frac{1}{T} \sum_{t=1}^{T} \left[\frac{x(t) - x_p(t)}{x(t)} \right]^2 \right\}^{\frac{1}{2}}.$$

and the normalised absolute mean difference is

$$\text{namd} = \frac{1}{T} \sum_{t=1}^{T} \left| \frac{x(t) - x_p(t)}{x(t)} \right|$$

where p denotes predicted in this case.

The delayed logistic map used in the present example is

$$x(t) = 3.8\, x(t-1) + \sum_{\sigma_1=1}^{\mu'} g_1'(\tau_1)\, x\,(t-\tau_1)$$

$$-3.8\, x^2(t-1) - \sum_{\sigma_1=1}^{\mu'} \sum_{\sigma_1=1}^{\mu'} g_2'(\tau_1,\tau_2)\, x\,(t-\tau_1)\, x\,(t-\tau_2) \qquad (15)$$

with an initial value $x(0) = 0.07839$, and a finite memory of $\mu'=6$. The response functions used are

$$g_1'(\tau_1) = 0.0145 \exp\{-(\tau_1-4)^2/9\} \qquad (16)$$

and

$$g_2'(\tau_1,\tau_2) = 0.010 \exp\{-0.3\tau_1\} \exp\{-0.3\tau_2\} \qquad (17)$$

respectively, and these may be seen as perturbations to the logistic map.

The moments of the sequence of data, $\{x(t)\}$, are then estimated. From these moments the response values deduced using equation (5). The autocovariances are estimated up to a maximum delay of $\tau_{max} = 8$. Equation (5) is then solved with N = 2 and for fixed delay values of $\mu = 1, 2, \ldots, 8$ respectively. In Table 1 the results of an analysis of the generated data are presented. As can be seen from the sample statistics in Table 1 the method correctly identifies the duration of memory of the mapping. In Table 2 the sample statistics between the original sequence and the modelled sequence are given. It should be emphasised that all of the

nonlinear response values, for $g_1(\tau_1)$ and $g_2(\tau_1,\tau_2)$ are solved simultaneously.

In this example it has been demonstrated that the moment formalism is able to correctly and accurately identify the order and form of the nonlinear mapping. The response values are a model of the time series data points and their utility is as a pragmatic tool with which predictions of future behaviour may be obtained rather than any insight into the nature of the process. To gain insights and understanding of the physical process the experimental design should be modified, where possible, such that the causal relationships may be established [21].

In order to test the predictive ability of the model coefficients two sequences of data were generated using the same initial condition, one sequence is generated using the estimated response values $g_1(\tau_1)$ and $g_2(\tau_1,\tau_2)$ and the other sequence generated using the actual response values $g'_1(\tau_1)$ and $g'_2(\tau_1,\tau_2)$. Figure 1 shows a sample of the predicted values $\{x_p(t)\}$ together with the observed sequence of data $\{x(t)\}$. In Figure 2 a plot of the common logarithm of the absolute difference between the two series, ie $|x_p(t) - x(t)|$, is given. As can be seen the divergence is exponential until the amplitude of the differences is the same as the envelope of $\{x(t)\}$ at which point chaos sets in and the limit of forward prediction has been reached. The gradient of the diverging difference is related to the Lyapunov exponent [1, 22].

TABLE 1: ANALYSIS OF ESTIMATED RESPONSE FROM DELAYED LOGISTIC MAP

Maximum Delay Considered	Estimated Area of Linear Function	rms Difference Linear Function	Estimated Volume of Quadratic Function	rms Difference Quadratic Function
1	3.884316	0.07236	-3.870614	0.06591
2	3.457699	0.4330	-3.3098321	0.2947
3	3.0929590	0.7235	-2.8170385	0.3948
4	2.6065230	0.5598	-2.1616390	0.3085
5	3.817648	0.7762	-3.7900739	0.3290
6	3.8680091	3.885×10^{-8}	-3.8569214	3.926×10^{-4}
7	1.889077	0.3190	-1.195642	0.1165
8	-0.27239	0.2542	1.71113	0.07773

TABLE 2: ANALYSIS OF TIME SERIES GENERATED USING THE ESTIMATED NONLINEAR RESPONSE VALUES

Maximum Delay Considered	Normalised Root Mean Square nrms	Normalised Absolute Mean Difference natnd
1	0.014267	0.0096923
2	0.010465	0.0066788
3	0.0073871	0.0041336
4	0.00648116	0.00369744
5	0.00293309	0.00166184
6	2.148×10^{-9}	6.011×10^{-10}
7	0.0040784	0.00098934
8	0.00826889	0.00193236

The formalism given by equation (5) has accurately identified the correct form of a nonlinear mapping when there is no noise present. The response values estimated from the data are able to predict the future time series values with a precision that is dependent on the Lyapunov exponent of the initial value problem. In practice the value of μ and the order N have to be determined in the analysis and may be considered as free parameters. The solution of equation (5) is, however, very sensitive to the value of μ and the order can be identified from a plot of $\{x(t)\}$ with $\{x_p(t)\}$ for deviations from a straight line which can indicate the presence of higher order terms.

Before the present work there was no exact method for isolating an individual nonlinear mapping and estimating its values. The above example

has demonstrated that it is possible to correctly identify the order, form and values of a nonlinear mapping in terms of response functions and to use the estimated response functions to predict the future behaviour of $\{x(t)\}$ to the limit defined by the intersection of the Lyapunov curve with the envelope of time series sequence.

WOLF'S SUNSPOT NUMBER

It has only been in recent years that nonlinear time series have been studied either systematically or in detail. Although many different approaches are being attempted, few have yet demonstrated utility and consistency where real data are concerned [11]. The development and testing of emerging techniques is aided by the availability of benchmark data sets on which the methods can be applied and assessed for their modelling and predictive ability. Wolf's sunspot number is such a benchmark data set [11].

The cycle of solar activity is evident in a plot of the mean number of sunspots observed on an annual basis. Several periods have been identified, but the 11.5 year cycle is the dominant one and formed the basis of much of the early understanding of solar and solar-terrestrial physics. The sunspots are convective cells near the surface of the sun's photosphere and in themselves do not represent a fundamental aspect of solar physics. However, the sunspot number is a suitable index that is easy to observe and which summarises the surface activity on the sun. The existence of sunspots has been known for 3000 years and its cyclic behaviour was established in 1843. Wolf made extensive investigations into the available historical astronomical records and organised the international effort to monitor the annual sunspot number, which now bears his name. The reliability of the sunspot number deteriorates with history prior to 1850 and is essentially unusable before 1710.

In the present work the sunspot number from 24 solar cycles, from 1710 to 1975, are used to characterise the annual sunspot number with nonlinear response values. These estimated response values are then used to predict the sunspot number in the 25th solar cycle, from 1976 to 1987. These predicted values are then compared against the observed sunspot numbers. In addition to the statistical aspects of model identification and

prediction the estimated response function values may be used to confirm if the annual sunspot number is a chaotic sequence. Yoshimura, in magnetohydrodynamic work [17] indicated that the sunspot number should be of a delayed quadratic logistic map form, that is, that there should be linear and quadratic nonlinear terms and that the quadratic response function should be diagonally dominated. The estimated values $g_1(\tau_1)$ and $g_2(\tau_1,\tau_2)$ represent a characterisation of the deterministic map form the data $\{x(t)\}$. The predictive power of this characterisation which together with the noise $\{r(t)\}$ is limited by the amplitude and form of the noise component. This is because the value of the estimated response functions will not be unique and the values are dependent on the assumed properties of the probability distribution. These are inherent weaknesses in the analyses of single series of data.

From the annual sunspot numbers, the linear and quadratic response values, $g_1(\tau_1)$ and $g_2(\tau_1,\tau_2)$ are estimated using equation (12) where again μ and $M_{rr}(0)$ are to be determined in the analysis.

Table 3 shows the values of the normalised root mean square differences between the 265 observed and modelled sunspot numbers for a range of fixed values of memory $9 \leq \mu \leq 14$ and noise variance $0.0 \leq M_{rr}(0) \leq 3.0$.

TABLE 3: NRMS Difference Values for the Sunspot Analysis

Fixed Delay Value μ	NRMS for variance of the noise $M_{rr}(0)$ values					
	0.00	0.01	0.10	1.00	1.25	3.00
9	1.050	1.058	1.064	1.097	1.103	1.066
10	1.047	1.055	1.051	1.042	1.103	1.281
11	1.066	1.074	1.054	1.069	1.076	1.213
12	1.026	1.027	1.024	1.035	1.039	1.085
13	1.116	1.110	1.083	1.066	1.066	1.067
14	1.066	1.065	1.053	1.077	1.081	1.073

On the basis of James' criteria [23], there is a shallow minimum which spans several time delay and variance values. For values of $M_{rr}(0) \geq 5.0$ the residuals diverged to infinity. The James' criteria can be used to estimate the standard error of the minimum as a function of the rate of divergence of the residuals in each dimension.

Table 4 shows the values of the normalised root mean square difference between the observed sunspot values from 1976 and the values predicted using the response functions estimated from the first 265 values.

TABLE 4: NRMS Difference Values for the Predicted Sunspot Numbers

Variance of Noise $M_{rr}(0)$	NRMS for fixed delay values μ					
	9	10	11	12	13	14
0.00	0.165	0.132	0.426	0.272	0.241	0.303
0.01	0.133	0.220	0.435	0.435	0.149	0.734
0.10	0.174	0.132	0.364	0.272	0.206	0.206
1.00	0.239	0.115	0.307	0.210	0.442	0.228
1.20	0.257	0.109	0.304	0.219	0.456	0.246
1.25	0.263	0.108	0.302	0.223	0.461	0.246
1.30	0.268	0.109	0.301	0.227	0.466	0.245
3.00	0.737	0.753	0.314	∞	∞	∞

where ∞ means greater than 10^{10}

Again there is a broad minimum, centred at μ = 10 and $M_{rr}(0)$ = 1.25, that spans a range of delay values, however, that is not surprising given the sample size. The standard error quoted on the annual sunspot number is 5% is a relative value for each observed number and this is not inconsistent with the value of 1.25 estimated for the whole sample of data. Figure 3 shows the modelled and observed sunspot number, and Figure 4 shows the predicted and observed sunspot number using the response values estimated when μ = 10 and $M_{rr}(0)$ = 1.25. As can be seen in Figures 3 and 4 the sunspot numbers are both modelled and predicted well, in addition, Figure 4 shows the sunspot number predictions extended up to 1991. The predicted annual sunspot number values are more accurate than previous linear and nonlinear autoregressive analyses [11]. For example, Figure 4 also shows the sunspot number predicted for 1991, given the data from 1710 to 1990. That sunspot value [24] was made using McNish's method [25] and agrees with the value for 1991 made with the formalism developed in this work which is effectively a 16 year prediction from 1975.

Figure 5 shows the response function values $g_1(\tau_1)$ and $g_2(\tau_1,\tau_2)$ estimated when μ = 10 and $M_{rr}(0)$ = 1.25. As can be seen the quadratic response values, $g_2(\tau_1,\tau_2)$, are diagonally dominated and so confirms Yoshimura's prediction of the form of the mapping being a delayed logistic map.

CHAOTIC BEHAVIOUR OF A DRIVEN NONLINEAR OSCILLATOR

Nonlinear electrical resonators are known to be a valuable means to investigate the properties of dynamic nonlinear systems. A simple series RLC nonlinear resonator is known to follow a bifurcation route [18] to fully developed chaos is studied. The nonlinear element in the circuit is a variactor diode, which under forward voltage conditions acts as a nonlinear voltage dependent capacitor. Several investigators have explored the phase space with spectral density methods [18, 26, 27] and have noted that the phase space has distinctly different regions. As yet these regions, have not yet been thoroughly experimentally investigated nor theoretically explained. Linsay [18], established the period doubling route to chaos and Testa et al [26] used spectral density measurements to confirm that the bifurcation diagram was that of a logistic map and that the convergence of the bifurcation sequence of voltages at a fixed driving frequency followed Feinbaum's universal scaling law [28]. In the present work the voltage values $\{x(t)\}$ observed across the inductive and capacitive components are analysed using the formalism developed in equation (11).

The nonlinear resonator circuit is a series array of a resistor, inductor and capacitor (RLC), in which the capacitor, a Motorola MV2108 variactor diode, is the non-linear component. The circuit was driven sinusoidally by an AIRMEC 304 frequency synthesiser which has an output impedance of 50Ω. The voltage across the capacitive and inductive components was considered as the output of the circuit, as in previous experiments using a circuit of this type [18, 29]. The time series sequences of voltage were recorded using a Gould DSO1604 20 MHz oscilloscope. The resonator circuit was as shown in reference [18], and the values of the components used were, resistance 180Ω, inductance 120μH and the capacitance of the diode is given approximately by

$$C(V_c) = \frac{C_o}{(1 - V_c/\phi)^{\mu}}$$

where C_o = 80pF, ϕ = 0.6V is the contact potential and μ is the junction gradient, which varies from 0.5 for an abrupt junction to 0.33 for a graded junction.

At low drive voltages the circuit behaved as a linear RLC circuit, as the drive voltage was increased, the circuit displayed the frequency multiplications observed by other investigators. As in previous investigations the bifurcation mode of 'phase' could be determined from displaying the input drive voltage versus the output voltage on the oscilloscope in the x-y mode and from the power spectral density of the time series displayed on the spectral analyser. The Lissajou figures displayed on the oscilloscope contained a number of loops equal to the bifurcation mode of 'phase' excited. Once a particular mode of phase space had been established, the real-time series input and output voltage signals were then captured by the digital oscilloscope and used to estimate the linear and non-linear response functions of the resonator circuit.

The frequency of the driving signal was set at 1.95MHz, and the voltage increased until a saturated chaotic state was obtained. The time series sequences of input and output voltage were captured and downloaded for analysis. The time series auto and cross moments of varying orders are estimated from a 1000 point sample of this time series data set, and from these the linear and quadratic response function values can be determined by the solution of equation (12), using standard matrix methods.

The order of a delayed logistic map is N = 2 and so the linear and quadratic response values were estimated from the representation

$$z(t) = r(t) + \sum_{\sigma_1=1}^{\mu} g_1(\sigma_1)x(t-\sigma_1) + \sum_{\sigma_1=1}^{\mu}\sum_{\sigma_2=1}^{\mu} g_2(\sigma_1,\sigma_2)x(t-\sigma_1)x(t-\sigma_2) \qquad (18)$$

and where the variance of $\{r(t)\}$, $M_{rr}(0)$, and the memory of the mapping, $1 \leq \mu \leq 10$, are to be determined in the analysis.

Table 5 shows the values of the normalised root mean square differences between the observed and modelled voltages for a range of fixed values of memory $1 \leq \mu \leq 10$ and variance $0.0 \leq M_{rr}(0) \leq 0.01$.

TABLE 5: NRMS Difference Values for the Electrical Circuit

Fixed Delay Value μ	NRMS for variance of the noise $M_{rr}(0)$ values					
	0.000	0.001	0.002	0.003	0.005	0.010
1	8.182	8.196	8.190	8.190	8.191	8.193
2	0.353	0.349	0.347	0.348	0.344	0.388
3	0.281	0.225	0.207	0.232	0.256	0.789
4	0.195	0.229	0.242	0.261	0.322	0.752
5	0.147	0.229	0.237	0.436	0.246	0.349
6	0.183	0.228	0.238	0.523	0.952	1.842
7	0.103	0.658	0.695	0.695	1.587	1.085
8	0.082	0.280	0.254	0.254	0.882	∞
9	0.094	0.176	0.620	0.620	5.790	∞
10	0.200	1.020	0.280	∞	∞	∞

(where ∞ means greater than 10^{10})

The least residual is for a noiseless mapping, ie when $M_{rr}(0) = 0.00$, however using the James criteria the width of the minimum is broad. Figure 6 shows a sample of the voltages observed and the voltages modelled using the estimated response functions clearly there is good agreement between the values. The response values estimated with the 1000 points of data are then used to predict the future behaviour of the voltage using the convolution

$$x(t) = \sum_{\sigma_1=1}^{\mu} g_1(\sigma_1)x(t-\sigma_1) + \sum_{\sigma_1=1}^{\mu}\sum_{\sigma_2=1}^{\mu} g_2(\sigma_1,\sigma_2)x(t-\sigma_1)x(t-\sigma_2)$$

given the initial conditions $\{x(t)\}$ for $(1000-\mu) \leq t \leq 1000$. The predicted values are then compared to the observed values in order to determine the nonlinear response functions' ability to determine the future behaviour.

Table 6 shows the values of the normalised root mean square differences between the observed values and the values predicted using the nonlinear response functions estimated from the first 1000 points of data. Figure 6 shows a sample of the observed and modelled voltages, clearly there is good agreement between the values.

TABLE 6: NRMS Difference Values for the Predicted Points

Fixed Delay Value μ	NRMS for variance of the noise $M_{rr}(0)$ values			
	0.000	0.001	0.002	0.003
1	1.078	1.078	1.078	1.078
2	0.153	0.155	0.157	0.162
3	0.132	0.138	0.132	∞
4	0.107	0.134	0.136	∞
5	0.098	0.176	0.181	∞
6	0.098	∞	∞	∞
7	0.083	∞	∞	∞
8	0.059	0.390	∞	∞
9	0.074	0.302	∞	∞
10	0.078	∞	∞	∞

The forward prediction is clearly more sensitive than the modelling. Figure 7 shows the predicted voltages for $\mu = 8$ and $M_{rr}(0) = 0.000$, together with the observed voltage values. The linear and quadratic response values at this point are given in Table 7.

Table 7: Estimated linear and quadratic response function values for the resonator circuit

	τ_1=1	τ_1=2	τ_1=3	τ_1=4	τ_1=5	τ_1=6	τ_1=7	τ_1=8
$g_1(\tau_1)$	1.503	-0.602	-0.134	-0.403	0.138	0.019	0.432	-0.504

$g_2(\tau_1,\tau_2)$	τ_2=1	τ_2=2	τ_2=3	τ_2=4	τ_2=5	τ_2=6	τ_2=7	τ_2=8
τ_1=1	0.204	-0.621	0.144	0.570	-0.478	0.023	-0.137	0.095
τ_1=2	-0.621	1.362	-0.495	-0.674	0.755	-0.195	0.005	0.140
τ_1=3	0.144	-0.495	0.713	-0.381	-0.258	0.376	-0.049	-0.109
τ_1=4	0.570	-0.674	-0.381	1.241	-0.533	-0.358	0.460	-0.141
τ_1=5	-0.478	0.455	-0.258	-0.533	0.367	0.164	-0.382	0.121
τ_1=6	0.022	-0.195	0.376	-0.358	0.164	0.298	-0.553	0.325
τ_1=7	-0.136	0.055	-0.049	0.459	-0.382	-0.553	0.896	-0.337
τ_1=8	0.095	0.140	-0.109	-0.141	0.120	0.325	-0.337	0.147

The estimated response values accurately characterise the properties of the data, see Figure 6, and correctly predict the behaviour of the voltage, see Figure 7; they do not, however, represent a logistic map as inferred by for example, Testa [26].

As mentioned above, the phase space of the electrical resonator has several different regions and that the different regions will have different solutions to the equations of motion. If this is the case then the response functions estimated in one region should not be able to predict the time series behaviour in another region. To test this hypothesis the driving voltage was reduced by three orders of magnitude and the frequency set at 2.5MHz. In this region of phase space the circuit acts as a linear RLC resonator.

The first, $\mu = 8$, values of the observed time series were used as the initial conditions for the prediction using the response functions estimated at fully developed chaos. Figure 8 shows a sample of the observed voltages and voltage values predicted using the response functions estimated at fully developed chaos. Figure 9 shows a similar comparison when the circuit is driven with white noise. As can be seen in both cases the estimated response functions yield reasonable predictions and the sample statistics are NRMS = 0.45 for the sinusoidal case and NRMS = 0.68 for the white noise case in Figure 9 indicated that the predicted values are good. Figure 9 also shows that the fundamental response of the varactor diode is shorter than 1μs, which is also evident if the input and output voltages are compared [29], and there is no evidence of the time constant $\tau = 2\pi/\omega$, invoked by Rollins and Hunt [30] to explain the finite memory, recovery time, of the diode at resonance.

Figure 10 shows the predicted time series values for another sample of white noise data the NRMS = 3.27 value indicates that the predictive power is poor for that case. As can be seen there are intermittent regions of the predicted sequence which 'remember' the form of the time series sequence used to estimate the response functions.

Thus, the estimated response functions are not consistent in their ability to predict the behaviour in different regions of phase space. They are local functions which are dependent on the form of forcing function used

when they were estimated. As this is the case, they should not be used to make inferences about the underlying physics of the process but may be used to characterise a particular data set and perform local predictions. In order to understand the underlying physics it is better, where possible, to modify the experimental design and obtain time series sequences of input and output data. The response functions estimated in that case are more global and are not dependent on the form of forcing function [24, 21].

CONCLUSIONS

The results presented in this paper can be summarised as follows. A formalism based on the Volterra series has been developed that will enable the identification and study of nonlinear systems of arbitrary order under the influence of a stochastic process. A set of nonlinear integral equations were developed in terms of statistical time series moments of the physical observable. An absolute moment form of the equation set was then used to demonstrate that it is possible to extract and isolate nonlinear response functions when the input data are drawn from a general nonlinear stochastic process. The numerical example used in this work was chosen to demonstrate the attributes of the formalism, in that is is able to accurately identify the form of the nonlinear mapping between time series points. Two sets of experimental data were then analysed using a mixed linear and quadratic form of mapping, because the data sets were predicted to be of a logistic map form by previous workers. The linear and quadratic response functions of Wolf's sunspot number were estimated from the time series moments. The form of the estimated response functions confirms Yoshimura's prediction that they should be governed by a delayed logistic map. These estimated response functions were then used to predict Wolf's sunspot number value from 1975. The predicted values were found to be better than previous linear and nonlinear autoregressive fits to the data [11]. The response functions for a series RLC circuit were then estimated from the time series voltage values. The linear and quadratic response functions estimated were able to predict the behaviour of the resonator under fully developed chaotic conditions and in a linear region of operation using the same form of forcing function and one white noise forcing function but not a second white noise sample. The response functions were not of a delayed logistic map form as inferred in previous work. This work has demonstrated that the formalism developed in equations

(5) and (11) can be used to characterise a particular sequence of data, however, the response functions estimated are local and forcing function dependent. This work has demonstrated that a single set of estimated response function values cannot characterise a wide region of the phase space of nonlinear physical situations. For this reason the analysis of single sequences of data are unlikely to yield insight into the fundamental physics underlying a nonlinear process. Where possible input and output sequences of data should be obtained and analysed.

ACKNOWLEDGEMENTS

This work was funded by the Building Sub-Committee of the UK Science and Engineering Research Council.

REFERENCES

[1] Oseledec V L, A Multiplicative Ergodic Theorem: Lyapunov Characteristic Numbers for Dynamic Systems, Trans. Moscow Math. Soc., 19, 1968, p 197-231

[2] Box G P E and Jenkins G M, Time Series Analysis Forecasting and Control, Holden Day, Oakland, California, 1976.

[3] Shraiman B, Wayne C E and Martin P C, Scaling Theory for Noisy Period-Doubling Transition to Chaos, Phys. Rev. Lett., 46, 1981, p 935-939.

[4] Testa J, Perez J and Jeffries C, Evidence for Chaotic Behaviour of a Nonlinear Driven Oscillator, Phys. Rev. Lett., 48, 1982, p 714-717.

[5] Abarbanel H D I, Brown H and Kodtke J B, Prediction in Chaotic Systems: Methods for Time Series with Broadband Fourier Spectra, Phys. Rev. A, 41, No. 4, 1990, p 1782-1807.

[6] Huberman B A and Zissok A B, Power Spectra for Strange Attractors, Phys. Rev. Lett., 46, 1981, p 626-628.

[7] Farmer J D, Spectral Broadening of Period-Doubling Bifurcation Sequences, Phys. Rev. Lett., 47, 1981, p 179-182.

[8] Nauemberg M and Rudnick J, Universality and the Power Spectrum at the Onset of Chaos, Phys. Rev. B, 24, 1981, p 493-495.

[9] Antonsen T M and Ott E, Multifractal Power Spectra of Passive Scalars Converted by Chaotic Fluid Flows, Phys. Rev. A, 44, 1990, p 951-857.

[10] Chan S and Billings S A, Representations of Nonlinear Systems: The NARMAX Model, Int. J. Control, Vol 49, No. 3, 1989, p 1013-1032.

[11] Tong H, Nonlinear Time Series: A Dynamic Systems Approach, Clarendon Press, Oxford, 1990.

[12] Broomhead D S and King G P, Extracting Qualitative Dynamics from Experimental Data, Physica D, 20, 1986, p 217-236

[13] Casdagli M, Nonlinear Prediction of Chaotic Time Series, Physica D, 35, 1989, p 335-356

[14] Farmer J D and Sidovowich J J, in Evolution Learning and Cognition, Edited by Y C Lee, World Scientific, 1988, p 277-330.

[15] Guckenheimer J and Holmes P, Nonlinear Oscillations Dynamical Systems and Bifurcations of Vector Fields, Springer Verlag, New York, 1983.

[16] Fick E, Fick M and Hausmann G, Logistic Equation with Memory, Phys. Rev. A, 44, 1991, p 2469-2473.

[17] Yoshimura H, The Solar-Cycle Period-Amplitude Relation as Evidence of Hysteresis of the Solar-Cycle Non-Linear Magnetic Oscillation and the Long-Term (55 year) Cycle Modulation, Astrophys. J., 227, 1979, p 1047-1058.

[18] Linsay P S, Period Doubling and Chaotic Behaviour in a Driven Anharmonic Oscillator, Phys. Rev. Lett., 47, 1981, p 1349-1352.

[19] Schaffer W M, Ellner S and Kot M, Effects of Noise on Some Dynamic Models in Ecology, J. Math. Biol., 1986, 24, p479-523.

[20] Volterra V, Theory of Functionals and of Integral and Integro-differential Equations, Dover, New York, 1959.

[21] Irving A D, Dewson T and Hong G, Nonlinear Response Estimation: I Inhomogeneous Case, Submitted to J. Phys. A, 1992.

[22] Campa A, Giansanti A and Tenenbaum A, Partial Lyapunov Exponents in Tangent Space Dynamics, J. Phys. A: Math. Gen., 25, 1992, p 1915-1924.

[23] James A N, Twin P J and Butler P A, The Statistical Analysis of γ-ray Angular Correlation Experiments, Nucl. Instru. and Methods, 115, 1974.

[24] Solar-Geophysical Data prompt reports, Jan 1991, Number 557, part 1.

[25] McNish A G and Lincoln J V, Trans. Am. Geophy. Union, 30, 1949, p 673-685.

[26] Testa J, Perez J and Jeffries, Evidence for Universal Chaotic Behaviour of a Driven Nonlinear Oscillator, Phys. Rev. Lett., 48, No. 11, 1982, p714-717.

[27] Baxter J H, Bocko M F and Douglas D H, Behaviour of a Nonlinear Resonator Driven at Subharmonic Frequencies, Phys. Rev. A, 41, No. 2, 1990, p619-625.

[28] Feigenbaum M J, Quantitative Universality for a Class of Nonlinear Transformations, J. Stat. Phys., 19, 1978, p25-52.

[29] Dewson T, Irving A D and Cunliffe N H, Nonlinear Response Estimation III: Analysis of a Nonlinear LCR Circuit, Submitted to J. Phys. A, 1992.

[30] Rollins R W and Hunt E R, Exactly Solvable Model of a Physical System Exhibiting Universal Chaotic Behaviour, Phys. Rev. Lett, 49, No. 18, 1982, p 1295-1298.

16 March 1991
Revised 18.5.1992
BB39a/ADI1

FIGURE CAPTIONS

Figure 1: Two sequences of data, using the same initial condition, one generated using the estimated response values, the other using the actual response values.

Figure 2: Plot, using logarithmic scale on the y axis, of the absolute difference between the predicted and observed time series shown in Figure 1.

Figure 3: Observed and modelled annual sunspot number for the years 1710-1975. The modelled values were calculated from the response function values estimated from this data.

Figure 4: Observed and predicted annual sunspot number for the 25th solar cycle. The predicted values are calculated from the response function values estimated by the formalism, from the 1710-1975 sunspot data.

Figure 5a: First order response function values $g_1(\tau_1)$ estimated by the formalism from Wolf's sunspot data.

Figure 5b: Second order response function $g_2(\tau_1, \tau_2)$ estimated by the formalism from Wolf's sunspot data.

Figure 6: A sample of the observed and modelled output voltage from the resonator circuit.

Figure 7: Observed and predicted output voltage from the circuit. The predicted values are calculated from the response function values estimated by the formalism, from a 1000 point sample of time series data.

Figure 8: Observed and predicted output voltage from the circuit in the linear region. The predicted values are calculated from the response function values estimated, by the formalism, in a fully developed chaotic region.

Figure 9: Observed and predicted voltage output from the circuit when driven by a noise source. The predicted values were calculated from the response function values estimated, by the formalism, in the fully developed chaotic region.

Figure 10: Observed and predicted voltage output from the circuit when driven by a noise source. The predicted values were calculated from the response function values estimated, by the formalism, in the fully developed chaos region.

BB39A

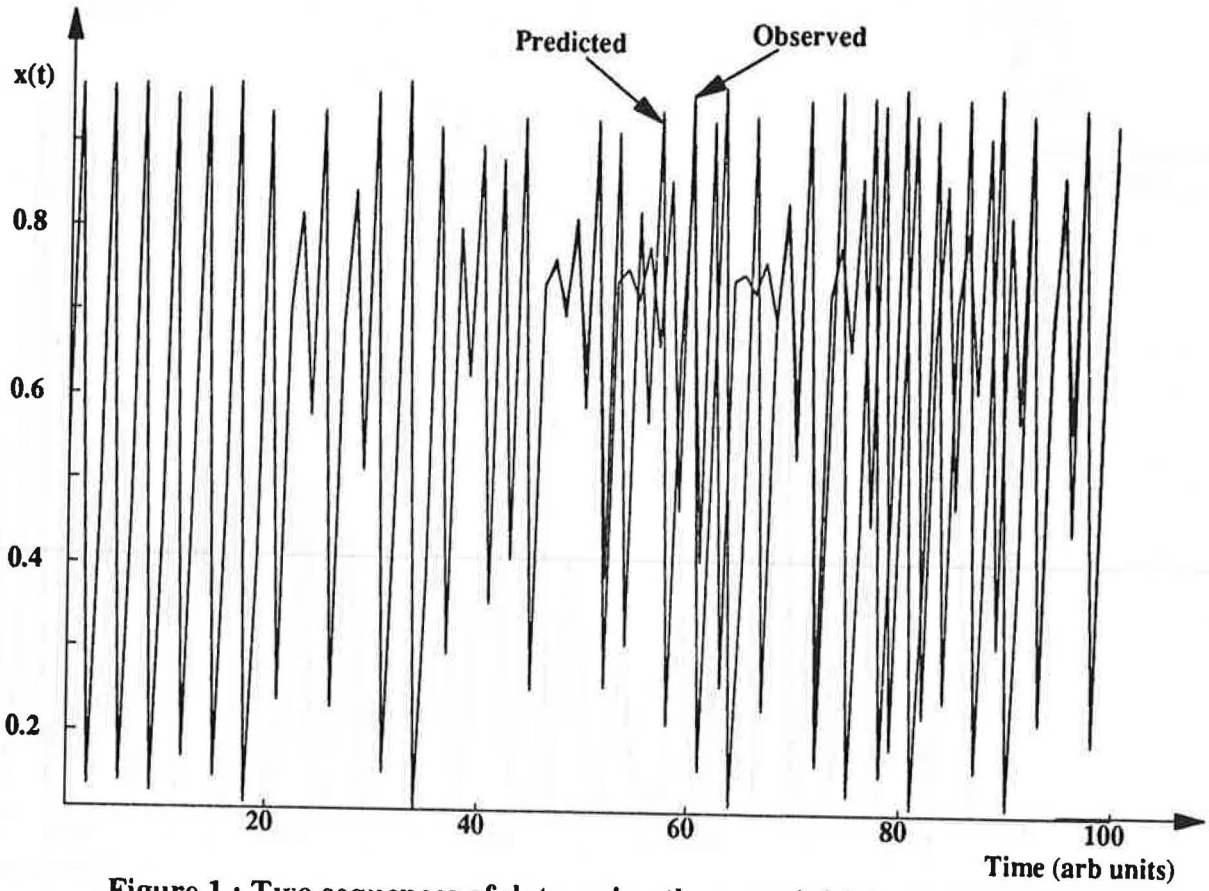

Figure 1 : Two sequences of data, using the same initial condition, one generated using the estimated response values, the other using the actual response values

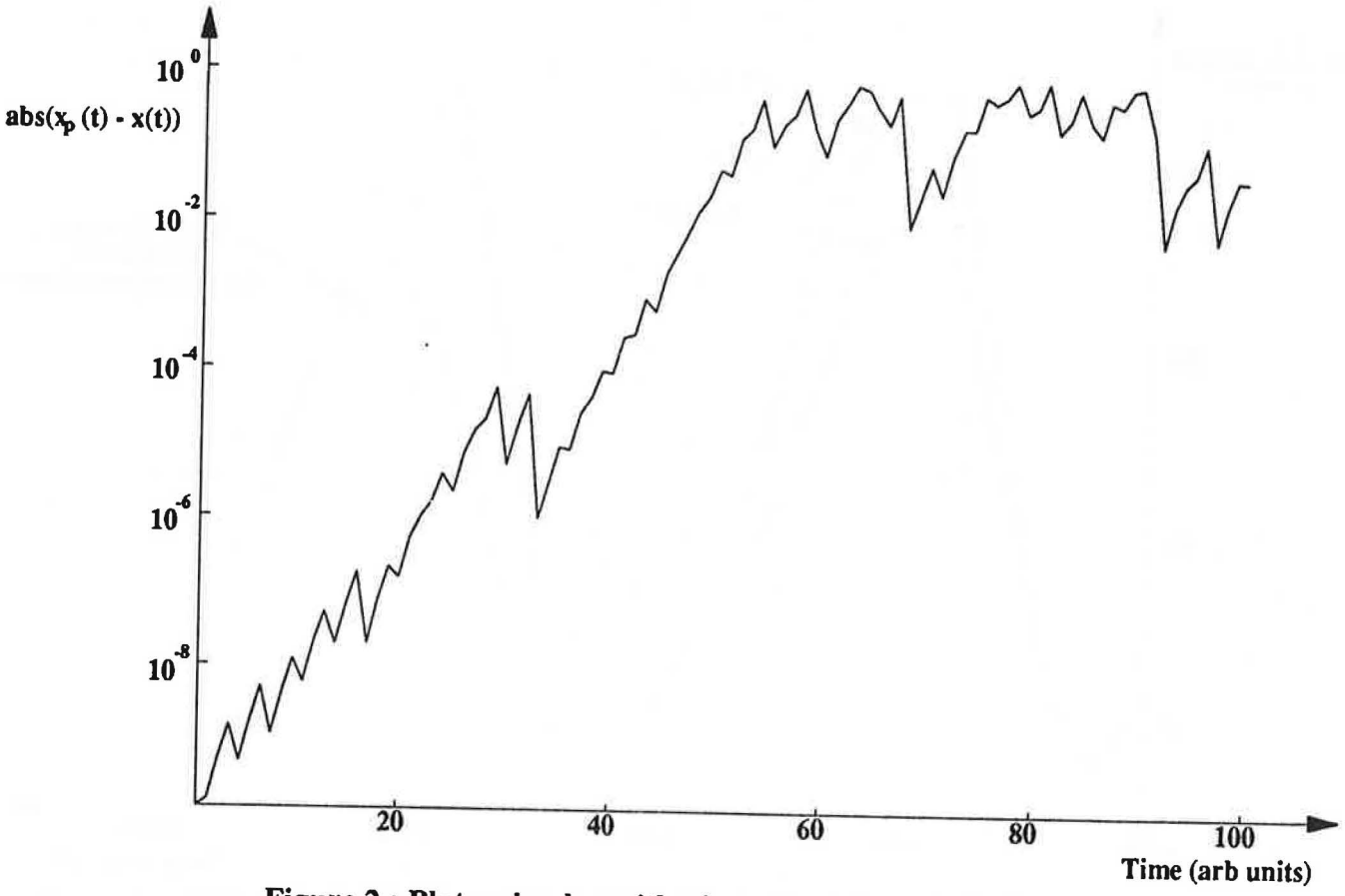

Figure 2 : Plot, using logarithmic scale on the y axis, of the absolute difference between the predicted and observed time series shown in figure 1

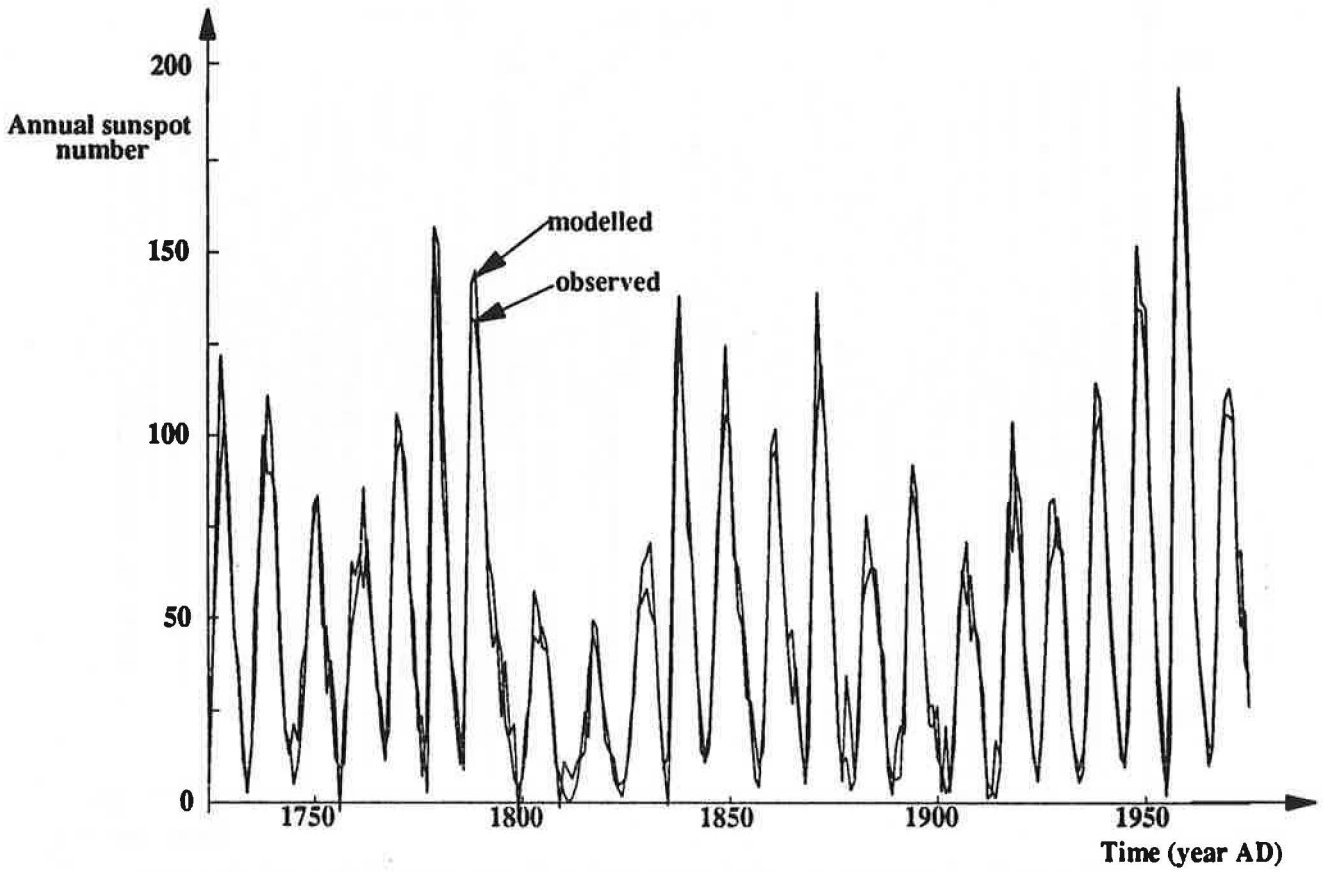

Figure 3 : Observed and modelled annual sunspot number for the years 1710-1975. The modelled values were calculated from the response function values estimated from this data

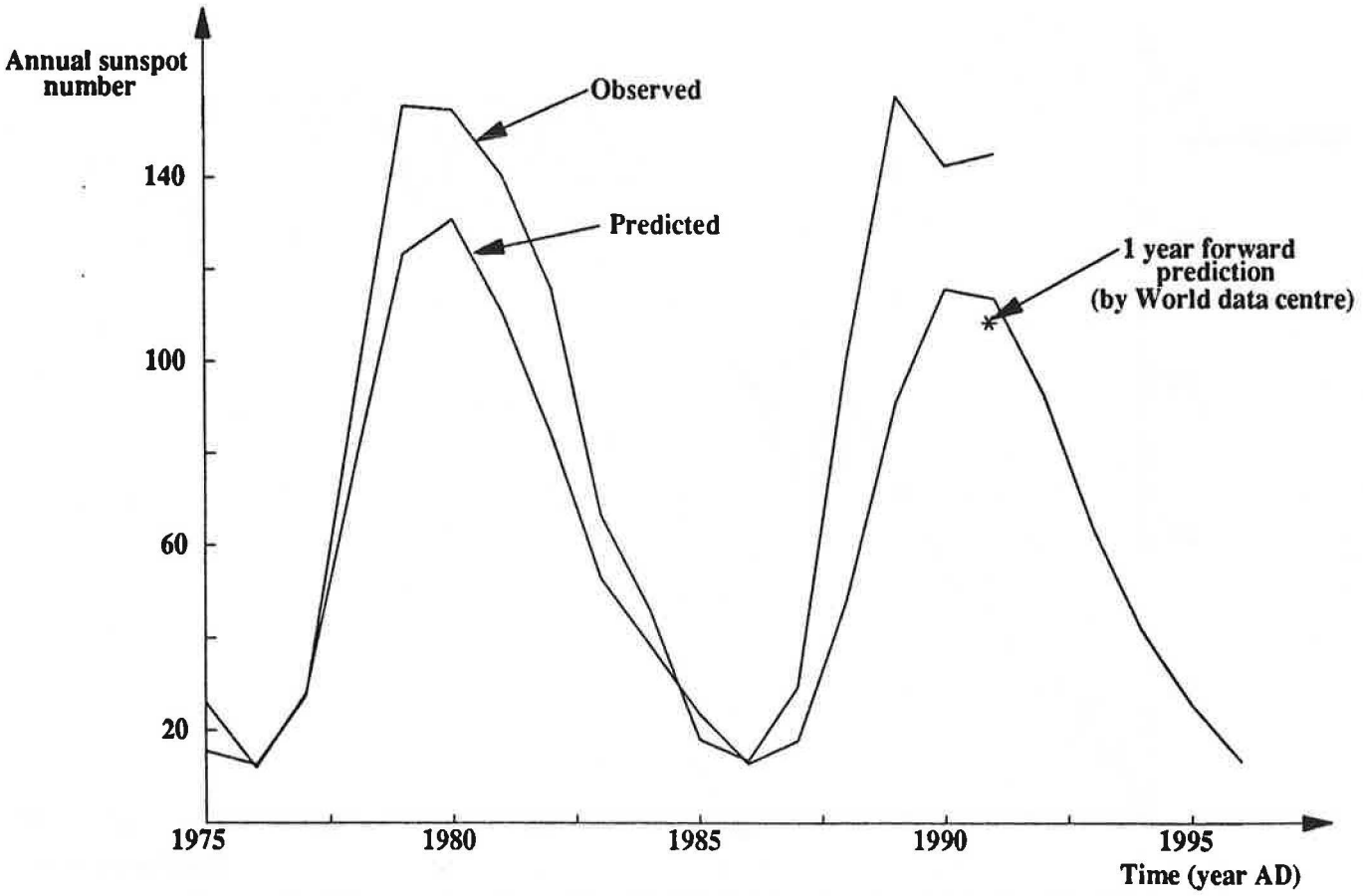

Figure 4 : Observed and predicted annual sunspot number for the 25th solar cycle The predicted values are calculated from the response function values estimated by the formalism, from the 1710-1975 sunspot data.

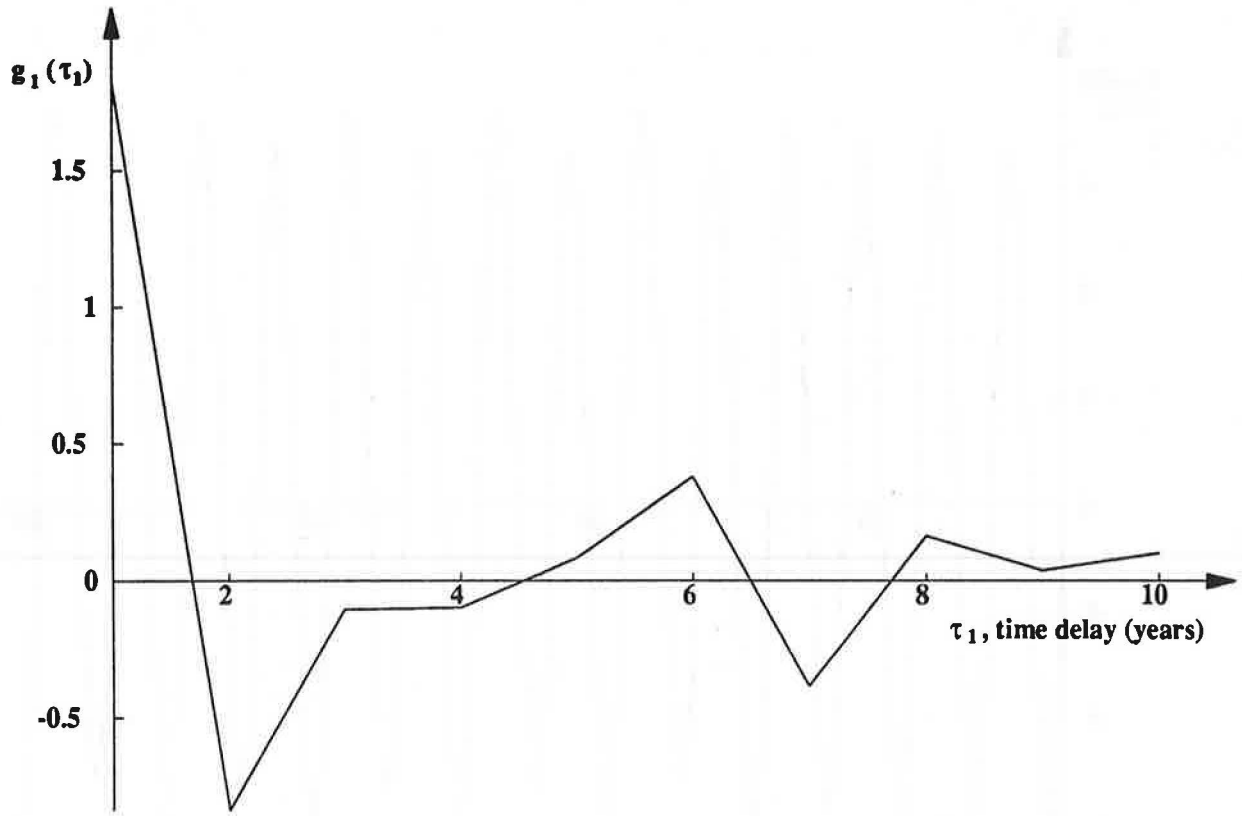

Figure 5a : First order response function values $g_1(\tau_1)$ estimated by the formalism from Wolf's sunspot data

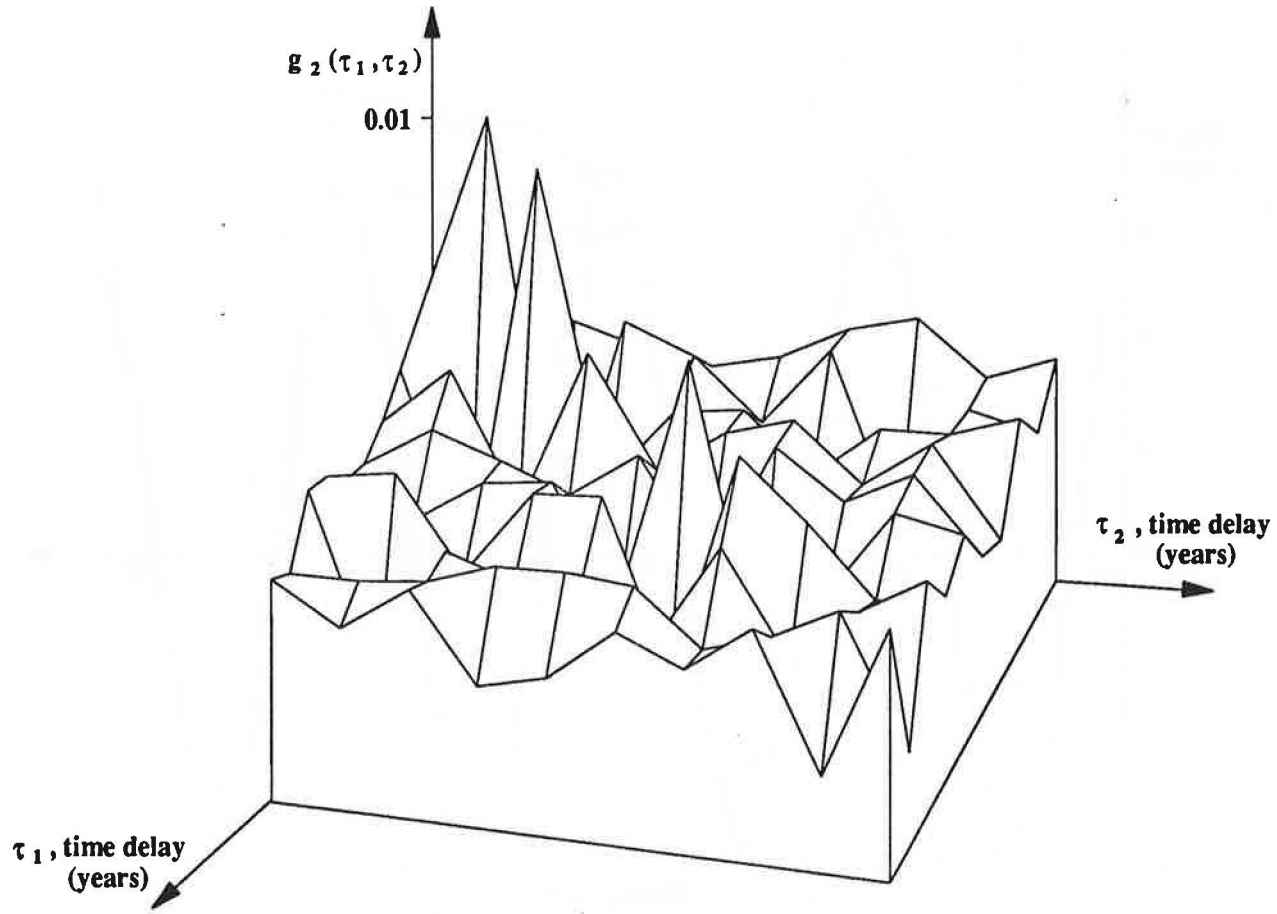

Figure 5b : Second order response function $g_2(\tau_1,\tau_2)$ estimated by the formalism from Wolf's sunspot data

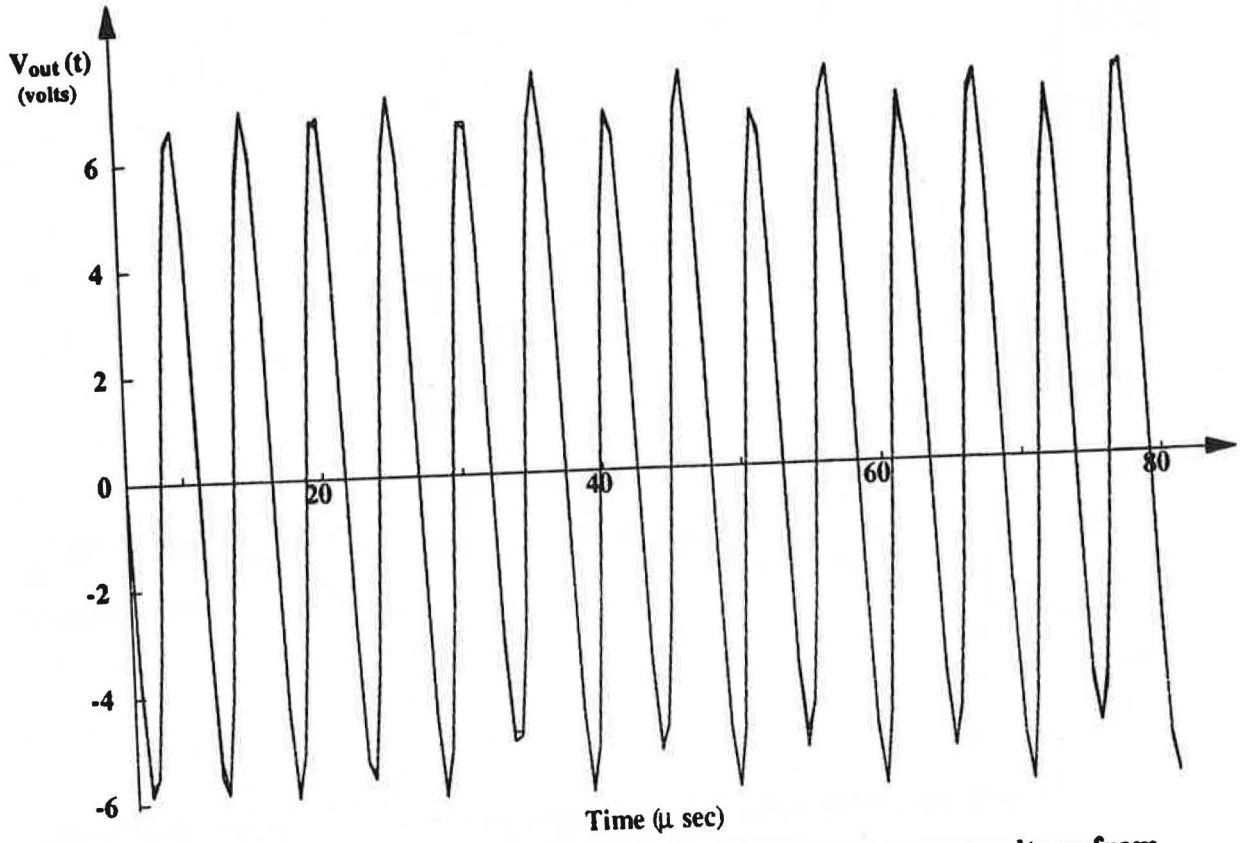

Figure 6 : A sample of the observed and modelled output voltage from the resonator circuit

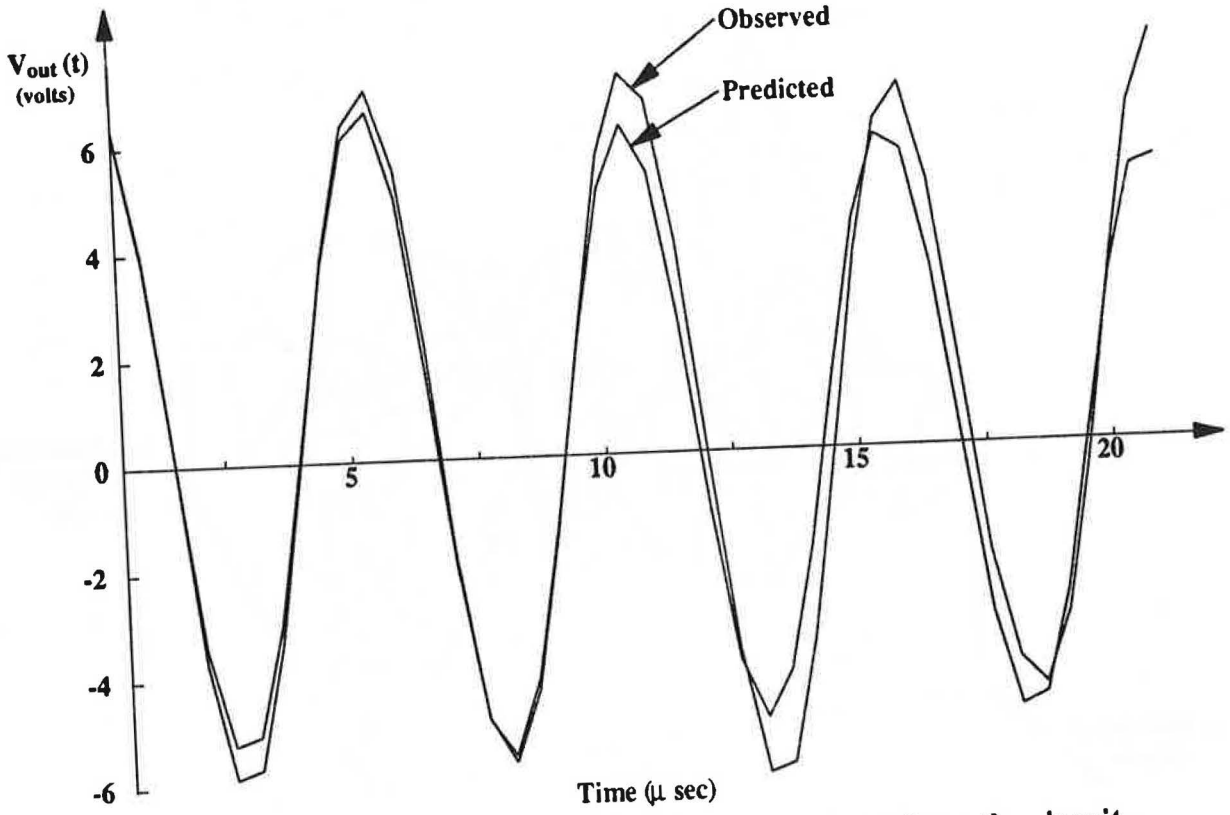

Figure 7 : Observed and predicted output voltage from the circuit. The predicted values are calculated from the response function values estimated by the formalism, from a 1000 point sample of time series data

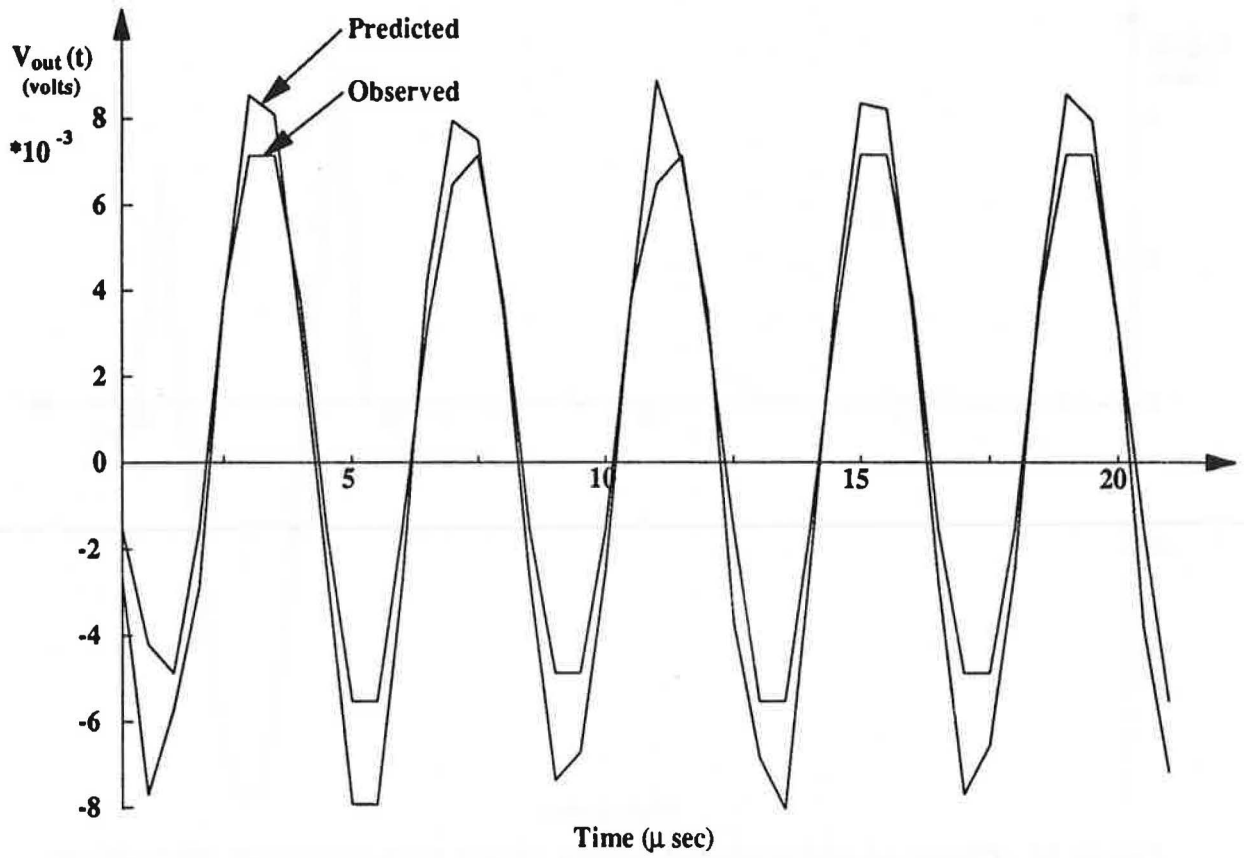

Figure 8 : Observed and predicted output voltage from the circuit in the linear region. The predicted values are calculated from the response function values estimated, by the formalism, in a fully developed chaotic region

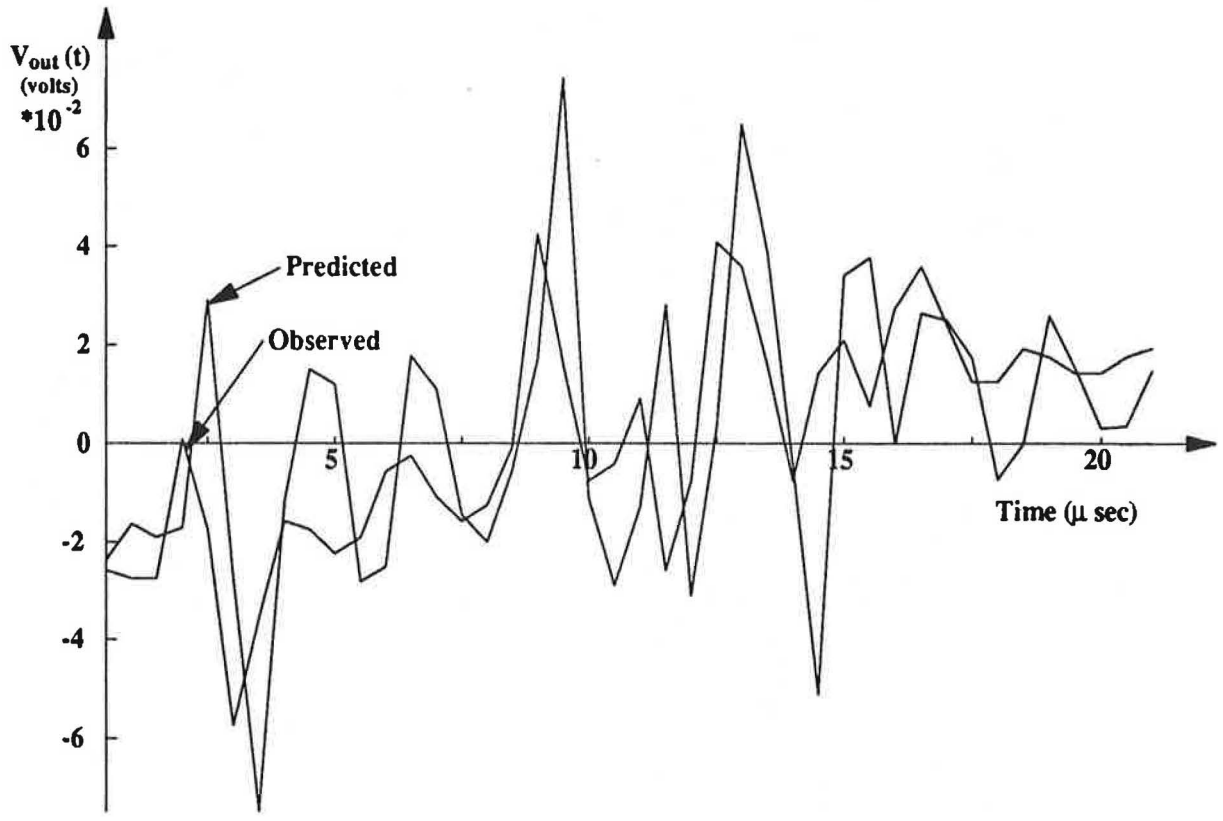

Figure 9 : Observed and predicted voltage output from the circuit when driven by a noise source. The predicted values were calculated from the response function values estimated, by the formalism, in the fully developed chaotic region

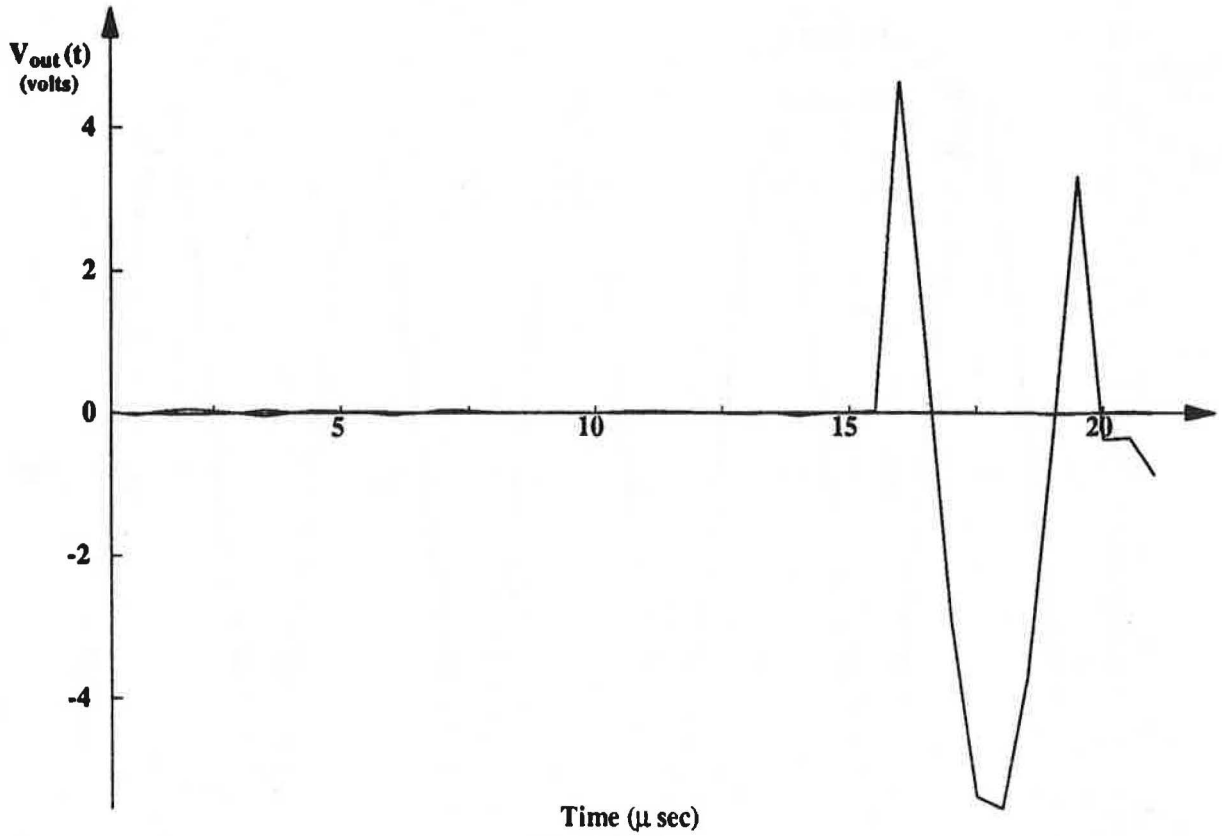

Figure 10 : Observed and predicted voltage output from the circuit when driven by a noise source. The predicted values were calculated from the response function values estimated, by the formalism, in the fully developed chaos region